

# Accounting for the photochemical variation of stratospheric NO<sub>2</sub> in the SAGE III/ISS solar occultation retrieval

Kimberlee Dubé<sup>1</sup>, Adam Bourassa<sup>1</sup>, Daniel Zawada<sup>1</sup>, Douglas Degenstein<sup>1</sup>, Robert Damadeo<sup>2</sup>, David Flittner<sup>2</sup>, and William Randel<sup>3</sup>

<sup>1</sup>Institute of Space and Atmospheric Studies, University of Saskatchewan, Saskatchewan, Canada

<sup>2</sup>NASA Langley Research Center, Hampton, VA, USA

<sup>3</sup>National Center for Atmospheric Research, Boulder, CO, USA

**Correspondence:** Kimberlee Dubé (kimberlee.dube@usask.ca)

**Abstract.** The Stratospheric Aerosol and Gas Experiment (SAGE) III has been operating on the International Space Station (ISS) since mid 2017. Nitrogen dioxide (NO<sub>2</sub>) number density profiles are routinely retrieved from SAGE III/ISS solar occultation measurements in the middle atmosphere. Although NO<sub>2</sub> density varies throughout the day due to photochemistry, the standard SAGE NO<sub>2</sub> retrieval algorithm neglects these variations along the instrument's line of sight by assuming that the number density has a constant gradient within a given vertical layer of the atmosphere. This assumption will result in a retrieval bias for a species like NO<sub>2</sub> that changes rapidly across the terminator. In this work we account for diurnal variations in retrievals of NO<sub>2</sub> from the SAGE III/ISS measurements, and determine the impact of this algorithm improvement on the resulting NO<sub>2</sub> number densities. The first step in applying the diurnal correction is to use publicly available SAGE III/ISS products to convert the retrieved number density profiles to optical depth profiles. The retrieval is then re-performed with a new matrix that applies photochemical scale factors for each point along the line of sight according to the changing solar zenith angle. In general NO<sub>2</sub> that is retrieved by accounting for these diurnal variations is more than 10% lower than the standard algorithm below 30 km. This effect is greatest in winter at high latitudes, and generally greater for sunrise occultations than sunset. Comparisons with coincident profiles from the Optical Spectrograph and InfraRed Imager System (OSIRIS) show that NO<sub>2</sub> from SAGE III/ISS is generally biased high, however the agreement improves by up to 20% in the mid stratosphere when diurnal variations are accounted for in the retrieval. We conclude that diurnal variations along the SAGE III/ISS line of sight are an important term to consider for NO<sub>2</sub> analyses at altitudes below 30 km.

*Copyright statement.* TEXT

## 1 Introduction

The Stratospheric Aerosol and Gas Experiment (SAGE) III on the International Space Station (ISS) uses solar occultation to measure the attenuation of sunlight through the middle atmosphere (Cisewski et al., 2014). These measurements are used to retrieve vertical profiles of nitrogen dioxide (NO<sub>2</sub>), as well as other atmospheric constituents, mainly ozone and aerosol

extinction coefficients. The SAGE III/ISS data complements that from the earlier SAGE II (McCormick, 1987) and SAGE III/Meteor-3M missions (Mauldin III et al., 1998), as well as data from limb-viewing instruments such as the Optical Spectrograph and Infrared Imager System (OSIRIS, Llewellyn et al., 2004), to provide a long-term record of NO<sub>2</sub>. It is important to have these data sets for understanding trends and variability in the stratosphere as NO<sub>2</sub> plays a role in the chemical depletion of the ozone layer. Several studies of the long-term trends and variability in NO<sub>2</sub> (Randel et al., 1999; Liley et al., 2000; Park et al., 2017; Galytska et al., 2019; Dubé et al., 2020) have shown a consistent increase in NO<sub>2</sub> and an associated decrease in O<sub>3</sub>.

NO<sub>2</sub> is mainly destroyed by photolysis so the concentration, or density, of NO<sub>2</sub> that is measured depends greatly on the position of the sun: there is a rapid decrease in NO<sub>2</sub> at sunrise and a rapid increase at sunset. During solar occultation measurements, such as those taken by SAGE III/ISS, the solar zenith angle (SZA) is 90° at the tangent point, but varies along the instrument's line of sight (LOS). The retrieved NO<sub>2</sub> profile has contributions from the full LOS, so it includes contributions from both the day and night sides of the Earth, which can have substantially different amounts of NO<sub>2</sub>. The existing SAGE III/ISS retrieval neglects variations in SZA along the LOS by assuming the concentration of NO<sub>2</sub> has a constant gradient at each altitude above the Earth's surface (SAGE III Algorithm Theoretical Basis Document, 2002). This is a source of systematic uncertainty in the retrieved NO<sub>2</sub> that has not been quantified for SAGE III/ISS. ~~Previous studies have~~

~~There have been several earlier cases in which diurnal variations were accounted for in NO<sub>2</sub> retrievals, for both space (e.g., Gordley et al., 1996) and ground-based instruments (e.g., Preston et al., 1997; Hendrick et al., 2004). Studies focused on occultation instruments have~~ examined the effect of ~~this the~~ variation in SZA ~~on retrieved from other occultation instruments along the LOS on retrieved~~ NO<sub>2</sub> profiles, and showed that ignoring it can result in a high bias, especially below 25 km (Gordley et al., 1996; Newchurch et al., 1996; Brohede et al., 2007). The purpose of this work is to account for diurnal variations along the LOS, assess the impact, and provide an improved SAGE III/ISS NO<sub>2</sub> data set for further study. This is done by adding correction factors to the retrieval that account for variations in NO<sub>2</sub> due to changing solar zenith angle along the LOS. By comparing the NO<sub>2</sub> concentration from this improved retrieval to that from the existing SAGE III/ISS retrieval it is possible to determine the importance of the photochemical effect. The results are also compared to NO<sub>2</sub> retrievals from OSIRIS limb scattering measurements to determine how the photochemical correction changes the bias between NO<sub>2</sub> products from the two different instruments.

## 2 NO<sub>2</sub> Photochemistry

The NO<sub>2</sub> number density depends on local solar time (LST) and equivalently, SZA (Figure 1). There is a sharp decrease in the NO<sub>2</sub> concentration at sunrise as NO<sub>2</sub> is photolyzed to become NO. Throughout the daylight hours NO<sub>2</sub> and NO are in approximate equilibrium. At sunset NO production ceases, resulting in a rapid increase in NO<sub>2</sub>. Overnight NO<sub>2</sub> decreases more slowly as it is converted to nitrogen-containing reservoir species. The exact shape of this diurnal cycle depends on altitude: the NO<sub>2</sub> concentration at 40 km stays roughly constant during the day and night, while at altitudes with more NO<sub>2</sub> there is a steady increase during the day and decrease at night.

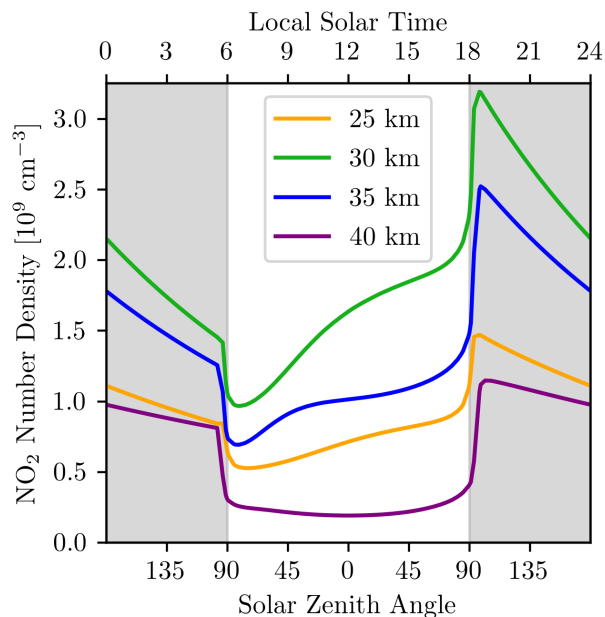


**Figure 1.** Daily cycle in  $\text{NO}_2$  at the equator as a function of local solar time (top axis) and solar zenith angle (bottom axis) for four altitudes.  $\text{NO}_2$  number density calculated with PRATMO photochemical box model.

55 The values in Figure 1 were calculated with the photochemical box model originally developed by Prather et al., 1992, which has been successively updated and is now often referred to as PRATMO (McLinden et al., 2000; Adams et al., 2017). PRATMO takes an input atmospheric state consisting of specified ozone, temperature, pressure, and air density profiles for a set latitude, longitude, and date. These input parameters are kept constant. The model then calculates a set of chemical reactions over a single day, iterating until the start and end values converge (Prather, 1992). This results in a 24 hour steady-state system of  
60 each species in the model. The model outputs are the  $\text{NO}_2$  profiles at any predetermined SZAs. These values can be used to scale the measured  $\text{NO}_2$  to different solar times in order to account for variations in SZA along the measurement LOS (Section 4). PRATMO scaling was used in several previous studies (e.g. Adams et al., 2017; Park et al., 2017; Dubé et al., 2020) to compare  $\text{NO}_2$  from instruments that measure at different times of day.

### 3 Instruments

#### 65 3.1 SAGE III/ISS

SAGE III has been in orbit on the ISS since March 2017. Level 2 data are available from June 2017 onwards. The ISS has an inclination of  $51.6^\circ$ , allowing SAGE III/ISS to view latitudes from  $70^\circ\text{N}$  to  $70^\circ\text{S}$ . The CCD spectrometer is configurable and currently observes wavelengths between  $\sim 280\text{nm}$  and  $\sim 1035\text{nm}$  with a resolution of 1-2nm. A separate photodiode covers  $\sim 1542\text{nm} \pm 15\text{nm}$ . During each occultation SAGE III/ISS continuously scans back and forth across the sun to measure the

70 irradiance. There are 15 sunrise and 15 sunset events per day. The coverage of SAGE III/ISS is very similar to that of SAGE II. The sunrise and sunset measurements progress in opposing directions, with each requiring about one month to achieve near global coverage.

The irradiances are used in the standard SAGE III/ISS retrieval (version 5.1, SAGE III Algorithm Theoretical Basis Document, 2002) to determine the number density of several species, as well as the aerosol extinction at several wavelengths. 75 The first step in the algorithm is to calculate slant path transmission profiles for each wavelength channel from the measured irradiance. Each slant path transmission profile is converted to a slant path optical depth profile that contains contributions from Rayleigh scattering, aerosol extinction, and absorption by at least one species. With this information  $\text{NO}_2$  and  $\text{O}_3$  slant path number density profiles are solved for simultaneously using multiple linear regression.  $\text{NO}_2$  is retrieved from channel S3, covering 433 to 450 nm. The slant path number density is converted to vertical number density profiles using a global fit 80 method that assumes each layer of the atmosphere is a spherical shell with a constant gradient. The final  $\text{NO}_2$  number density is available from 10 to 45 km on a 0.5 km grid with a vertical resolution of about 1.5 km. The reported uncertainty in the SAGE III/ISS  $\text{NO}_2$  is around 5% at 30 km, and increases to up to 20% at 10 km and 40 km. This uncertainty is due to measurement noise only, and does not account for systematic bias due to the horizontal homogeneity assumption.

### 3.2 OSIRIS

85 OSIRIS has been in sun-synchronous orbit on the Odin satellite since October 2001 (Murtagh et al., 2002; Llewellyn et al., 2004). There are 100 to 400 vertical profiles of limb-scattered solar irradiance measured each day, at wavelengths from 280 to 800 nm.  $\text{NO}_2$  is retrieved by spectral fitting in the wavelength range from 435 to 477 nm for altitudes from the cloud top to 39.5 km with a resolution of 2 km.

Earlier versions of the OSIRIS  $\text{NO}_2$  retrieval were developed by Haley et al. (2004), Bourassa et al. (2011), and Sioris et al. 90 (2017). The most recent data, version 7.0, is used here for validation of SAGE III/ISS  $\text{NO}_2$ . Version 7.0 improves upon version 6.0 by using solar Fraunhofer lines to fit the spectral point spread function of OSIRIS rather than using pre-flight calibration values. Cloud and aerosol discrimination is also refined to better detect cloudy scenes and to push the retrieval farther into the UTLS (Upper Troposphere Lower Stratosphere) following the method of Rieger et al. (2019).

The OSIRIS LOS is approximately aligned with the terminator so the variation in SZA along the LOS is much smaller than 95 for occultation instruments. McLinden et al. (2006) studied the effect of the diurnal error on  $\text{NO}_2$  from OSIRIS and found that it is only significant when the SZA is near  $90^\circ$  and the solar azimuth angle varies significantly from  $90^\circ$ . These extreme conditions occurred in 16% of profiles from 2004, resulting in errors of up to 35% in the OSIRIS  $\text{NO}_2$  below 25 km. Sioris et al. (2017) used PRATMO to create a 2D OSIRIS  $\text{NO}_2$  retrieval to further assess the impact of diurnal variations on the results. They found minimally improved agreement between OSIRIS  $\text{NO}_2$  and  $\text{NO}_2$  from balloon measurements, particularly below 100 20 km. Owing to the minimal effect for OSIRIS, the standard  $\text{NO}_2$  data product is produced neglecting the  $\text{NO}_2$  photochemical gradient.

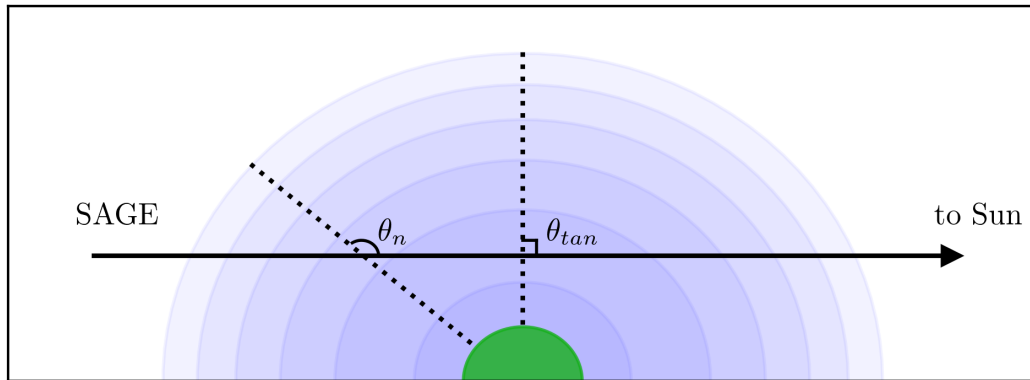


**Figure 2.** Geometry of a SAGE III occultation. The green semi-circle represents the Earth, and the blue semi-circles represent layers of the atmosphere. The angle  $\theta_{tan}$  is the SZA at the tangent point, and the angle  $\theta_n$  is the SZA angle for a shell at altitude  $n$ .

#### 4 Retrieval

During each occultation SAGE III/ISS looks through multiple layers of the atmosphere, called shells. Each shell is defined by its altitude. Figure 2 illustrates this geometry. The black arrow represents the LOS, pointing from the instrument to the sun.

105 The SZA at a given location is the angle between the dotted line and the LOS. At the tangent point this angle,  $\theta_{tan}$ , is  $90^\circ$ . For some other shell with an altitude  $n$  the SZA  $\theta_n$  is greater than  $90^\circ$  on the instrument side of the tangent point, as shown in the Figure. For this same shell altitude the SZA is less than  $90^\circ$  on the sun side of the tangent point.

The SAGE III/ISS retrieval assumes that the number density of each chemical constituent is either constant or has a constant gradient within a shell (SAGE III Algorithm Theoretical Basis Document, 2002). This assumption is generally valid for  
 110 species such as ozone that undergo minimal diurnal variation in the stratosphere, however it is not true for  $\text{NO}_2$ . This can be understood by considering Figure 3. For both lines of sight in the figure the SZA at the tangent point is  $90^\circ$ . To retrieve the  $\text{NO}_2$  concentration at the tangent point of a given LOS we need to know the  $\text{NO}_2$  concentration at each shell altitude that the LOS passes through. For example, the retrieved  $\text{NO}_2$  at 22 km depends on the  $\text{NO}_2$  at 32 km. The  $\text{NO}_2$  at 32 km is retrieved at the tangent point, where the SZA is  $90^\circ$ , but the 22 km line of sight passes through the 32 km shell when the SZA is around  
 115  $86.8^\circ$  on the near side of the tangent point and  $93.2^\circ$  on the far side (left panel of Figure 3). The right panel of Figure 3 shows that the  $\text{NO}_2$  concentration at 32 km and the two SZAs where the 22 km LOS passes through that shell are both different from the concentration when the SZA is  $90^\circ$ . In addition, the  $\text{NO}_2$  does not change linearly across the terminator so deviations from linearity on either side of the LOS do not cancel out. Therefore using the 32 km  $\text{NO}_2$  at  $90^\circ$  to retrieve the 22 km  $\text{NO}_2$  is inaccurate, and it cannot be assumed that the number density has a constant gradient across the terminator within a layer of the  
 120 atmosphere when performing the retrieval. This lack of spherical homogeneity can be accounted for by adding factors to the retrieval that scale the  $\text{NO}_2$  according to SZA, at each location along the LOS.

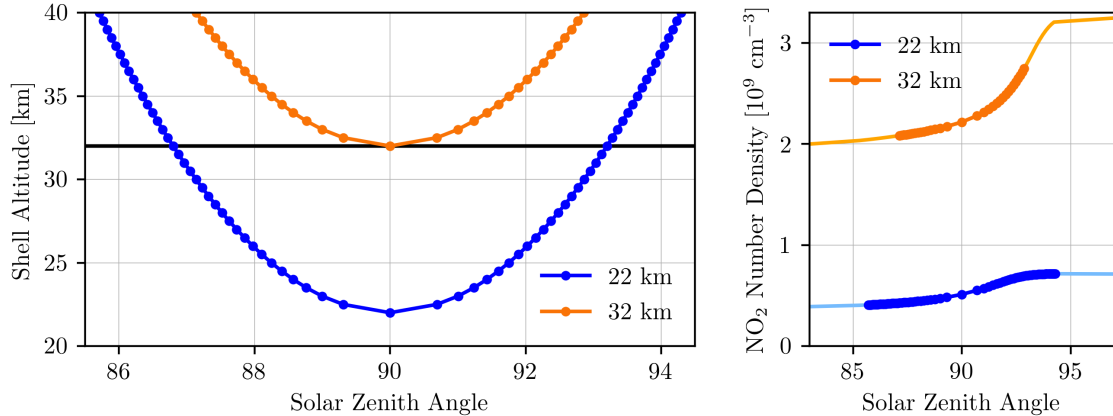


**Figure 3.** Left: Change in SZA with shell altitude along two lines of sight for a simulated sunset occultation. Right: Change in NO<sub>2</sub> at tangent altitudes of 22 km and 32 km for the same simulated sunset occultation. The dark, dotted lines correspond to the lines of sight from the left panel.

Ideally we would incorporate the scale factors by redoing the conversion of slant path optical depth, obtained directly from the solar transmission measurements, to number density. As the SAGE III/ISS NO<sub>2</sub> optical depth profiles are not publicly available, we instead start by undoing the SAGE III/ISS retrieval to revert the number densities to optical depths. This is done  
 125 using the matrix equation,

$$\tau = \sigma X_0 n_0, \tag{1}$$

where  $\tau$  is the vertical profile of slant path optical depths from NO<sub>2</sub>,  $\sigma$  is the NO<sub>2</sub> cross section, and  $n_0$  is the number density profile.  $X_0$  is the path length matrix where each row represents a LOS for a particular tangent point altitude and each column represents a different altitude through which the LOS passes. Each element of  $X_0$  is the path length distance between  
 130 subsequent shells along the LOS. The path lengths on opposite sides of the tangent point are the same (i.e. the distance from shell 1 to 2 on the instrument side of the tangent point is the same as the distance from shell 1 to 2 on the sun side) which allows  $X_0$  to be written as an upper triangular matrix where values from opposite sides of the tangent point are added together.

These optical depths are used to find the number densities accounting for diurnal variations,  $n_{dv}$ , using a new matrix,  $X_{dv}$ ,

$$n_{dv} = \sigma^{-1} X_{dv}^{-1} \tau. \tag{2}$$

135 In this matrix each path length includes a factor, explained below, that depends on the SZA at that location. Note that the NO<sub>2</sub> cross section is the same in both equations 1 and 2 and so it cancels out when finding  $n_{dv}$ . Although this is not strictly the case, using a constant cross section is a reasonable approximation as the cross section has a weak temperature and pressure dependence. The equations also assume that optical depth is constant within each layer of the atmosphere.

For a given SAGE III/ISS scan we know the date and time, the tangent point position, the spacecraft position, and the NO<sub>2</sub>  
 140 number density from the SAGE v5.1 retrieval. This information is all that is needed to construct  $X_0$ . To build the matrix we

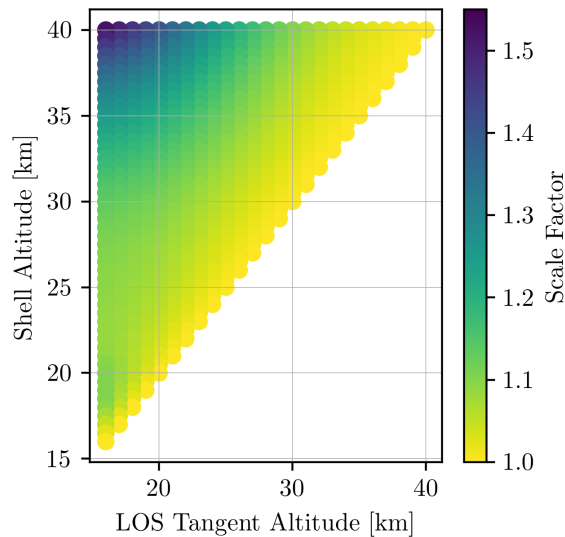


**Figure 4.** Scale factor matrix for a sunset occultation at the equator in March, simulated with PRATMO. The scale factors from either side of the tangent point are added to together, resulting in an upper triangular matrix.

iterate through each LOS, moving from the tangent point to the top of the atmosphere. The LOS is the vector from the satellite to the tangent point. The effect of refraction is neglected as it is small at the altitudes being considered.

The LOS for a particular tangent altitude intersects all of the shells above it. To find the scale factors for a given LOS we first find the apparent local solar time at the midpoint of each path created by the intersection of that LOS with the shells. PRATMO is then run with input ozone, temperature, and pressure from the SAGE III/ISS Level 2 scan data. The model NO<sub>2</sub> is computed at each calculated LST and at a SZA of 90°, corresponding to the exact time of sunrise or sunset. For each shell altitude along the LOS, the scale factor is the PRATMO NO<sub>2</sub> at that altitude (corresponding to the LST at that location) divided by the PRATMO NO<sub>2</sub> at the tangent point altitude for that LOS (the scale factor is 1 for the shell containing the tangent point). There is no scaling done above 40 km as the low amount of NO<sub>2</sub> can lead to unphysically large scale factors, despite small absolute differences in NO<sub>2</sub> along the LOS. The uncertainty in the SAGE III/ISS NO<sub>2</sub> also becomes large above 40 km and we want to prevent abnormal values from influencing the results at lower altitudes.

Figure 4 shows the photochemical scale factor matrix for a simulated event. The values in the figure are not multiplied by the path lengths. The matrix is created such that the scale factors from opposite sides of the tangent point need to be added together. This results in a scale factor that is equal to one along the diagonal, corresponding to unscaled values at the tangent point, and greater than one everywhere else. The scale factors increase as the path length component of the LOS gets further away from the tangent point.

It is also useful to look at the scale factor as a function of altitude along each LOS (Figure 5). Lower lines of sight pass through more layers of the atmosphere, resulting in greater scale factors. For lines of sight below about 30 km the change in scale factor with altitude becomes non-linear. This is because the shape of NO<sub>2</sub> cycle across the terminator changes with

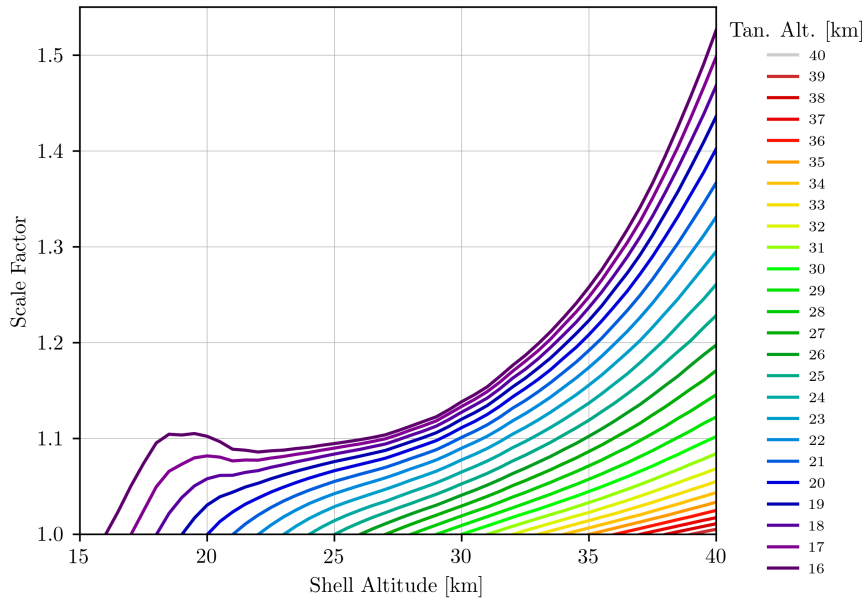


**Figure 5.** Scale factors along each line of sight for a sunset occultation at the equator in March, simulated with PRATMO.

160 altitude (right panel of Figure 3). At higher altitudes the  $\text{NO}_2$  increases along the whole LOS; below about 30 km the  $\text{NO}_2$  starts to level out on the night-side (the curve on either side of the terminator becomes different), changing the slope of the scale factor curves in Figure 5.

The scaled path length matrix,  $X_{dv}$ , is equal to the initial path length matrix,  $X_0$ , where each element has been multiplied by the corresponding element from the scale factor matrix shown in Figure 4.  $X_{dv}$  is used along with the calculated slant path  
 165 optical depths in Equation 2 to get the  $\text{NO}_2$  number density, accounting for diurnal variations. The resulting values of  $n_{dv}$  will be smaller than the original retrieved values. This is because the gradient on the near side of the LOS is smaller than the gradient on the far side, resulting in scale factors greater than one and therefore lower  $\text{NO}_2$ . Figure 6 shows the results for a sample SAGE III/ISS event. The left panel contains the optical depth profile, while the center panel compares the SAGE III/ISS  $\text{NO}_2$  number density with the diurnally varying number density, and the right panel shows the percent difference between the  
 170 two number density profiles. For this SAGE III/ISS event the percent difference between the two profiles becomes greater as altitude decreases to 17 km. Below this point the difference starts to become smaller again.

## 5 Results

The effect of accounting for diurnal variations on the retrieved SAGE III/ISS  $\text{NO}_2$  is quantified by the difference between the SAGE v5.1 retrieval and the diurnally varying retrieval (Figure 7). In general the difference between the retrievals becomes  
 175 greater than 20% below 25 km, which is larger than the reported random uncertainty in the SAGE III/ISS  $\text{NO}_2$ . Including the diurnal variations is more important in the winter at high latitudes; at these times the relative  $\text{NO}_2$  decrease at sunrise/increase



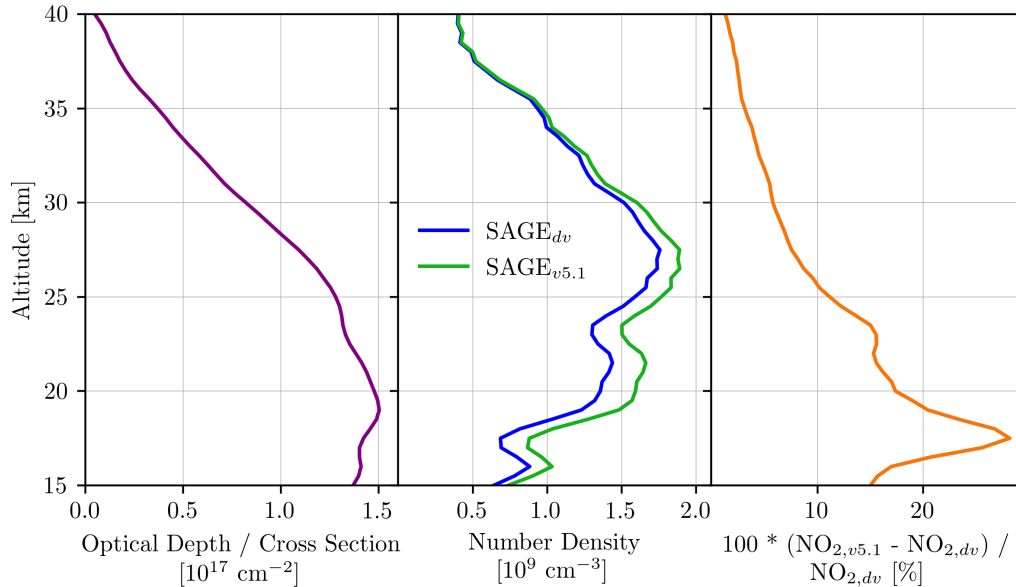


**Figure 6.** Left: NO<sub>2</sub> optical depth. Centre: NO<sub>2</sub> number density for both the diurnally varying and SAGE v5.1 retrievals. Right: Percent difference between the two number density profiles. Calculated for SAGE III/ISS event 967110.

at sunset is larger. The bias between the retrievals is not consistent between the sunrise and sunset NO<sub>2</sub> due to the differences in NO<sub>2</sub> chemistry at these times. This can be seen by looking at Figure 1: the change in NO<sub>2</sub> across the terminator has a different shape at sunrise than at sunset. Including diurnal variations along the LOS in the retrieval has a greater effect on sunrise than sunset above 25 km in the tropics and everywhere at higher latitudes.

The results presented in Figure 7 are very similar to those in Brohede et al. (2007), where they estimated the magnitude of neglecting diurnal variations in NO<sub>2</sub> for a simulated occultation instrument (not specific to SAGE II or III). They found that the bias increases rapidly below 25 km (below the peak in NO<sub>2</sub> density) and is larger at low latitudes for sunset. They also found that at high latitudes the bias is largest near equinoxes and sunrise values are slightly larger than sunset values. It was determined that this effect was enough to explain most of the difference between SAGE III/Meteor-3M and OSIRIS NO<sub>2</sub> at low altitudes (although they did not actually apply the correction to the SAGE III/Meteor-3M data).

The magnitude of the photochemical effect is also similar to that used in the Halogen Occultation Experiment (HALOE, Russell III et al., 1993) retrieval. HALOE is one occultation instrument that does include diurnal effects in the retrieval (Gordley et al., 1996). They use a factor based on results from the previous layer and a model that provides the NO<sub>2</sub> mixing ratio as a function of SZA and season. This is less accurate than the scale factors used in the present study, which are modelled for each NO<sub>2</sub> profile individually. The effect of the HALOE scaling is considered significant below 25 hPa ( $\approx$  27 km). They also

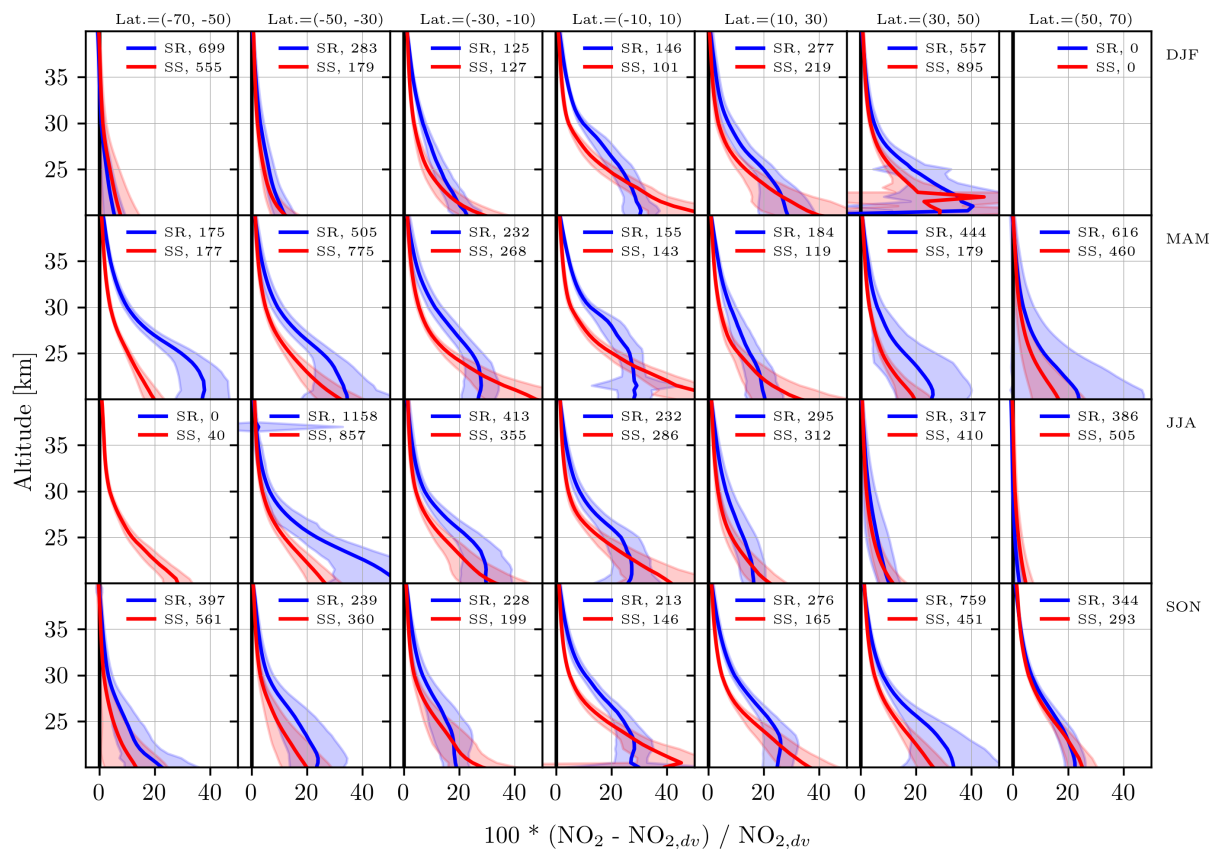


**Figure 7.** Mean difference between the SAGE v5.1 and diurnally varying (dv) retrievals for SAGE III/ISS sunset and sunrise  $\text{NO}_2$ . The error bars are the standard deviation.  $\text{NO}_2$  values more than five standard deviations from the mean are not included.

found the diurnal effect in sunrise to be 2-3 times larger than in sunset, which is greater than the difference between sunrise and sunset observed here for SAGE III/ISS.

Accounting for diurnal variations in the retrieval changes the SAGE III/ISS  $\text{NO}_2$  time series. This is shown in Figure 8 for several latitude bins at 25.5 km. The sunset  $\text{NO}_2$  number density decreases by about 5% to 20%, with the largest decreases occurring in the tropics. The effect of the diurnal variations on the sunrise  $\text{NO}_2$  has a more pronounced seasonal cycle than sunset, with a greater decrease in the winter, and a difference ranging from 5% to 30%. During winter months the diurnal effect is about 2 times greater at sunrise than at sunset, which is comparable to the difference reported for HALOE  $\text{NO}_2$  in Gordley et al. (1996). However during the summer the bias is similar for both sunrise and sunset. These variations in the time series should be considered when using the SAGE III/ISS  $\text{NO}_2$  data.

Both the diurnally varying and SAGE v5.1 retrievals were compared with OSIRIS  $\text{NO}_2$  as a way to validate the data (panel a of Figure 9). Only the morning (ascending node) OSIRIS measurements are used as a drift in the OSIRIS orbit affects the descending node sampling. The comparisons were done for events within 24 hours,  $10^\circ$  longitude, and  $2^\circ$  latitude, although

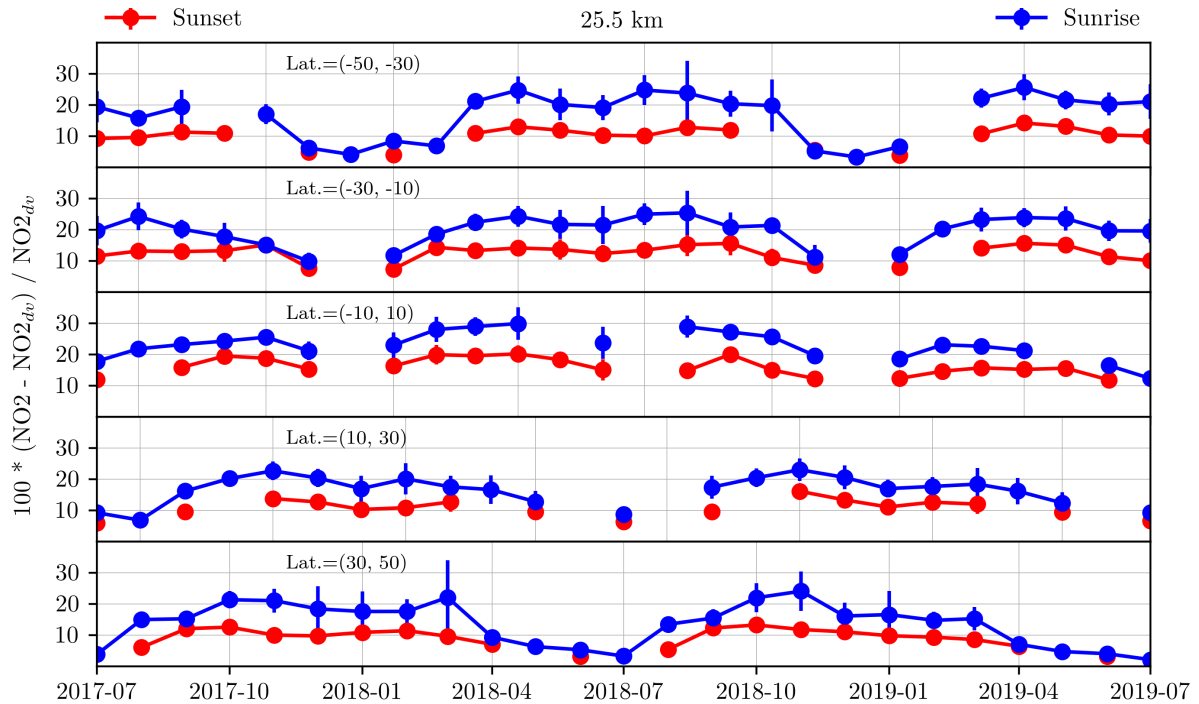


**Figure 8.** Mean difference between the SAGE v5.1 and diurnally varying ( $dv$ ) retrievals for SAGE III/ISS sunset and sunrise  $\text{NO}_2$  at 25.5 km. The error bars are the standard deviation.

the exact choice of coincidence criteria has minimal effect on the results. The SAGE III/ISS profiles were shifted from sunrise  
 205 and sunset to the OSIRIS measurement time using PRATMO. The SAGE III/ISS  $\text{NO}_2$  is generally biased high compared to the OSIRIS  $\text{NO}_2$ , with a difference of up to 50% at low altitudes/high latitudes. The differences between SAGE III/ISS and OSIRIS are within the combined uncertainties of the instruments. In general the SAGE III/ISS sunrise measurements agree better with OSIRIS than sunset, which could be because OSIRIS measures close to sunrise. The comparison was also performed excluding OSIRIS profiles with a SZA angle greater than  $86^\circ$ , where the diurnal effect is significant. This had a negligible effect on the  
 210 difference with SAGE III/ISS.

Accounting for diurnal variations in the SAGE III/ISS retrieval improves agreement with OSIRIS by up to 20% in the mid-stratosphere (panel b of Figure 9). Overall the diurnally varying SAGE III/ISS  $\text{NO}_2$  agrees better with the OSIRIS  $\text{NO}_2$  than the SAGE v5.1  $\text{NO}_2$ . The only region where this is not true is near the tropical tropopause. This area is where the diurnal effect becomes large (Figure 7), resulting in much smaller SAGE III/ISS  $\text{NO}_2$  values. The sunset  $\text{NO}_2$  in particular decreases by up  
 215 to 50% below 25 km in the tropics. This is larger than the initial difference between SAGE III/ISS and OSIRIS, resulting in the negative bias that is observed from 15 to 25 km at low latitudes.

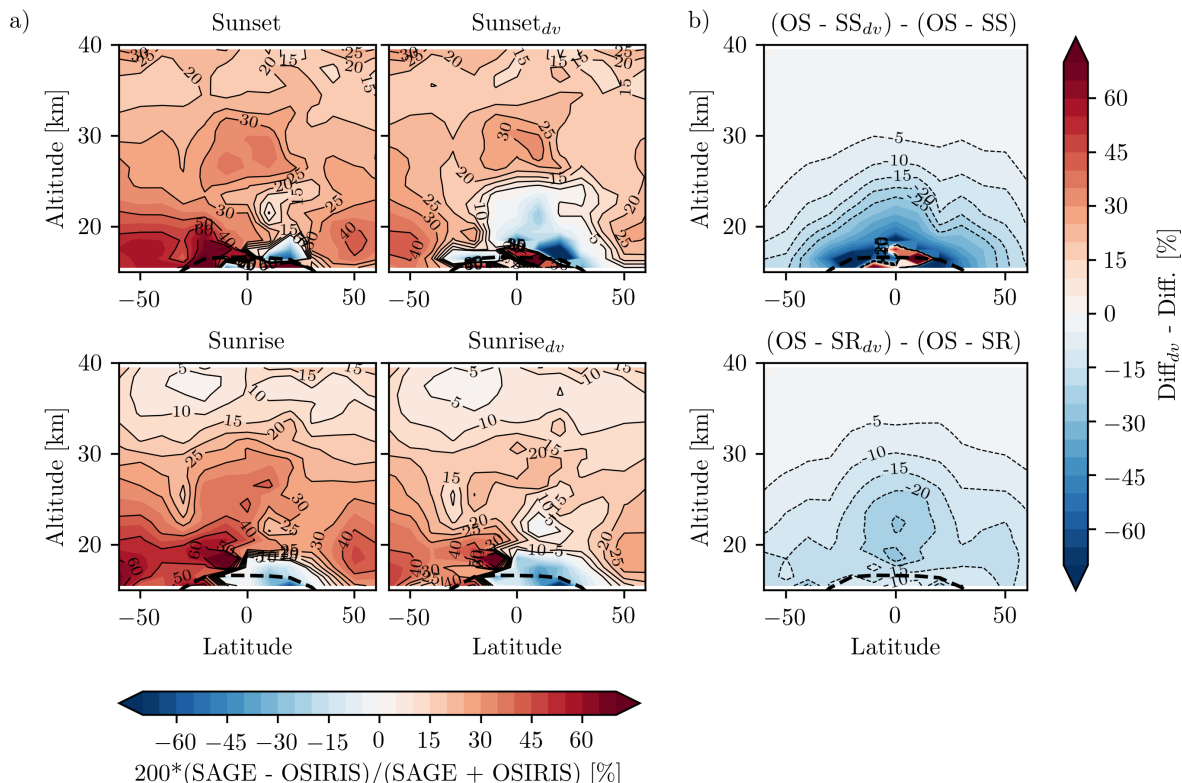


**Figure 9.** Panel a: Zonal mean percent differences of SAGE III/ISS sunset and sunrise  $\text{NO}_2$  and OSIRIS  $\text{NO}_2$  coincident measurements for the SAGE v5.1 and diurnally varying ( $dv$ ) retrievals. The contour spacing is 5%. The bold dashed line is the mean tropopause location. Panel b: Difference between the columns in panel a.

## 6 Conclusions

We have developed a retrieval algorithm that uses publicly available SAGE III/ISS data to account for changes in  $\text{NO}_2$  along the occultation line of sight that come from the photochemically driven diurnal cycle. The retrieval relies upon scaling factors  
 220 derived from a photochemical box model with input ozone, temperature, and pressure profiles taken from the reported SAGE III/ISS scan.

It was determined that the neglect of diurnal variations in the SAGE v5.1 retrieval always biases the results high. Note that this high bias is present in  $\text{NO}_2$  retrieved from any occultation instrument that neglects diurnal variability. In the case of SAGE III/ISS  $\text{NO}_2$ , we found that carefully accounting for diurnal variations in the retrieval is quite important below 30 km, with an  
 225 effect nearing 20% on the resulting values. The correction has the greatest effect at high winter latitudes, and is more important for sunrise occultations than sunset. These are potentially important differences in the reported  $\text{NO}_2$  densities in the lower stratosphere, where several interesting chemical and dynamical science questions remain. Including diurnal variations in the

NO<sub>2</sub> retrieval also has an impact on the monthly zonal mean time series which should be considered when studying long term variability.

230 Accounting for these diurnal variations in the SAGE III/ISS retrieval improves the agreement with OSIRIS NO<sub>2</sub> by up to 20% at lower altitudes. While there is a remaining bias between SAGE III/ISS and OSIRIS that is not well understood, it has a reasonable magnitude considering the very different measurement and retrieval techniques, and is within their combined uncertainties.

*Data availability.* The SAGE III/ISS Level 1 and 2 data are available through <https://search.earthdata.nasa.gov/>. The SAGE III/ISS NO<sub>2</sub> 235 that was retrieved by accounting for diurnal variations is available at <https://research-groups.usask.ca/osiris/data-products.php>. OSIRIS NO<sub>2</sub> is also available at the previous link.

*Author contributions.* KD performed the analysis and prepared the manuscript. DZ assisted with writing the retrieval code. AB and DD proposed the original idea for the project and provided guidance throughout. RD provided assistance with using the SAGE III/ISS data. DF and WR, along with the other authors, provided significant feedback on the analysis and the manuscript.

240 *Competing interests.* The authors declare that they have no conflicts of interest.

*Acknowledgements.* The authors thanks the Swedish National Space Agency and the Canadian Space Agency for the continued operation and support of Odin-OSIRIS. We also thank the SAGE III/ISS science team for providing the SAGE III/ISS data. SAGE III/ISS is a NASA Langley managed Mission funded by the NASA Science Mission Directorate within the Earth Systematic Mission Program. Enabling partners are the NASA Human Exploration and Operations Mission Directorate, International Space Station Program and the European Space Agency. 245 The National Center for Atmospheric Research is sponsored by the US National Science Foundation. [We thank Emmanuel Dekemper and one anonymous referee for their helpful comments on the manuscript.](#)

## References

- Adams, C., Bourassa, A. E., McLinden, C. A., Sioris, C. E., von Clarmann, T., Funke, B., Rieger, L. A., and Degenstein, D. A.: Effect of volcanic aerosol on stratospheric NO<sub>2</sub> and N<sub>2</sub>O<sub>5</sub> from 2002–2014 as measured by Odin-OSIRIS and Envisat-MIPAS, *Atmospheric Chemistry and Physics*, 17, 8063–8080, <https://doi.org/10.5194/acp-17-8063-2017>, 2017.
- 250 Bourassa, A. E., McLinden, C. A., Sioris, C. E., Brohede, S., Bathgate, A. F., Llewellyn, E. J., and Degenstein, D. A.: Fast NO<sub>2</sub> retrievals from Odin-OSIRIS limb scatter measurements, *Atmospheric Measurement Techniques*, 4, 965–972, <https://doi.org/10.5194/amt-4-965-2011>, <https://www.atmos-meas-tech.net/4/965/2011/>, 2011.
- Brohede, S. M., Haley, C. S., McLinden, C. A., Sioris, C. E., Murtagh, D. P., Petelina, S. V., Llewellyn, E. J., Bazureau, A., Goutail, F., 255 Randall, C. E., et al.: Validation of Odin/OSIRIS stratospheric NO<sub>2</sub> profiles, *Journal of Geophysical Research: Atmospheres*, 112, 2007.
- Cisewski, M., Zawodny, J., Gasbarre, J., Eckman, R., Topiwala, N., Rodriguez-Alvarez, O., Cheek, D., and Hall, S.: The Stratospheric Aerosol and Gas Experiment (SAGE III) on the International Space Station (ISS) Mission, in: *Sensors, Systems, and Next-Generation Satellites XVIII*, vol. 9241, p. 924107, International Society for Optics and Photonics, 2014.
- Dubé, K., Randel, W., Bourassa, A., Zawada, D., McLinden, C., and Degenstein, D.: Trends and Variability in Stratospheric NO<sub>x</sub> Derived 260 From Merged SAGE II and OSIRIS Satellite Observations, *Journal of Geophysical Research: Atmospheres*, 125, e2019JD031 798, 2020.
- Galytska, E., Rozanov, A., Chipperfield, M. P., Dhomse, Weber, M., Arosio, C., Feng, W., and Burrows, J. P.: Dynamically controlled ozone decline in the tropical mid-stratosphere observed by SCIAMACHY, *Atmospheric Chemistry and Physics*, 19, 767–783, <https://doi.org/10.5194/acp-19-767-2019>, <https://www.atmos-chem-phys.net/19/767/2019/>, 2019.
- Gordley, L., Russell III, J., Mickley, L., Frederick, J., Park, J., Stone, K., Beaver, G., McInerney, J., Deaver, L., Toon, G., et al.: Validation of 265 nitric oxide and nitrogen dioxide measurements made by the Halogen Occultation Experiment for UARS platform, *Journal of Geophysical Research: Atmospheres*, 101, 10 241–10 266, 1996.
- Haley, C. S., Brohede, S. M., Sioris, C. E., Griffioen, E., Murtagh, D. P., McDade, I. C., Eriksson, P., Llewellyn, E. J., Bazureau, A., and Goutail, F.: Retrieval of stratospheric O<sub>3</sub> and NO<sub>2</sub> profiles from Odin Optical Spectrograph and Infrared Imager System (OSIRIS) limb-scattered sunlight measurements, *Journal of Geophysical Research: Atmospheres*, 109, <https://doi.org/10.1029/2004JD004588>, <https://agupubs.onlinelibrary.wiley.com/doi/abs/10.1029/2004JD004588>, 2004.
- 270 Hendrick, F., Barret, B., Van Roozendaal, M., Boesch, H., Butz, A., De Mazière, M., Goutail, F., Hermans, C., Lambert, J.-C., Pfeilsticker, K., and Pommereau, J.-P.: Retrieval of nitrogen dioxide stratospheric profiles from ground-based zenith-sky UV-visible observations: validation of the technique through correlative comparisons, *Atmospheric Chemistry and Physics*, 4, 2106, 2004.
- Liley, J. B., Johnston, P. V., McKenzie, R. L., Thomas, A. J., and Boyd, I. S.: Stratospheric NO<sub>2</sub> variations from a long time series at 275 Lauder, New Zealand, *Journal of Geophysical Research: Atmospheres*, 105, 11 633–11 640, <https://doi.org/10.1029/1999JD901157>, <https://agupubs.onlinelibrary.wiley.com/doi/abs/10.1029/1999JD901157>, 2000.
- Llewellyn, E. J., Lloyd, N. D., Degenstein, D. A., Gattinger, R. L., Petelina, S. V., Bourassa, A. E., Wiensz, J. T., Ivanov, E. V., McDade, I. C., Solheim, B. H., McConnell, J. C., Haley, C. S., von Savigny, C., Sioris, C. E., McLinden, C. A., Griffioen, E., Kaminski, J., Evans, W. F., Puckrin, E., Strong, K., Wehrle, V., Hum, R. H., Kendall, D. J., Matsushita, J., Murtagh, D. P., Brohede, S., Stegman, J., Witt, G., 280 Barnes, G., Payne, W. F., Piché, L., Smith, K., Warshaw, G., Deslauniers, D. L., Marchand, P., Richardson, E. H., King, R. A., Wevers, I., McCreath, W., Kyrölä, E., Oikarinen, L., Leppelmeier, G. W., Auvinen, H., Mégie, G., Hauchecorne, A., Lefèvre, F., de La Nöe, J., Ricaud, P., Frisk, U., Sjöberg, F., von Schéele, F., and Nordh, L.: The OSIRIS instrument on the Odin spacecraft, *Canadian Journal of Physics*, 82, 411–422, <https://doi.org/10.1139/p04-005>, 2004.

- Mauldin III, L. E., Salikhov, R., Habib, S., Vladimirov, A. G., Carraway, D., Petrenko, G., and Comella, J.: Meteor-3M (1)/Stratospheric  
285 Aerosol and Gas Experiment III (SAGE III) jointly sponsored by the National Aeronautics and Space Administration and the Russian  
Space Agency, in: *Optical Remote Sensing of the Atmosphere and Clouds*, vol. 3501, pp. 355–365, International Society for Optics and  
Photonics, 1998.
- McCormick, M.: Sage II: An overview, *Advances in Space Research*, 7, 219 – 226, [https://doi.org/https://doi.org/10.1016/0273-1177\(87\)90151-7](https://doi.org/https://doi.org/10.1016/0273-1177(87)90151-7), <http://www.sciencedirect.com/science/article/pii/0273117787901517>, 1987.
- 290 McLinden, C. A., Olsen, S. C., Hannegan, B., Wild, O., Prather, M. J., and Sundet, J.: Stratospheric ozone in 3-D models: A simple chemistry and the cross-tropopause flux, *Journal of Geophysical Research: Atmospheres*, 105, 14 653–14 665, <https://doi.org/10.1029/2000JD900124>, 2000.
- McLinden, C. A., Haley, C. S., and Sioris, C. E.: Diurnal effects in limb scatter observations, *Journal of Geophysical Research: Atmospheres*, 111, 2006.
- 295 Murtagh, D., Frisk, U., Merino, F., Ridal, M., Jonsson, A., Stegman, J., Witt, G., Eriksson, P., Jiménez, C., Megie, G., Noë, J. d. I., Ricaud, P., Baron, P., Pardo, J. R., Hauchcorne, A., Llewellyn, E. J., Degenstein, D. A., Gattinger, R. L., Lloyd, N. D., Evans, W. F., McDade, I. C., Haley, C. S., Sioris, C., Savigny, C. v., Solheim, B. H., McConnell, J. C., Strong, K., Richardson, E. H., Leppelmeier, G. W., Kyrölä, E., Auvinen, H., and Oikarinen, L.: An overview of the Odin atmospheric mission, *Canadian Journal of Physics*, 80, 309–319, <https://doi.org/10.1139/p01-157>, <https://doi.org/10.1139/p01-157>, 2002.
- 300 Newchurch, M. J., Allen, M., Gunson, M. R., Salawitch, R. J., Collins, G. B., Huston, K. H., Abbas, M. M., Abrams, M. C., Chang, A. Y., Fahey, D. W., Gao, R. S., Irion, F. W., Loewenstein, M., Manney, G. L., Michelsen, H. A., Podolske, J. R., Rinsland, C. P., and Zander, R.: Stratospheric NO and NO<sub>2</sub> abundances from ATMOS Solar-Occultation Measurements, *Geophysical Research Letters*, 23, 2373–2376, <https://doi.org/10.1029/96GL01196>, <https://agupubs.onlinelibrary.wiley.com/doi/abs/10.1029/96GL01196>, 1996.
- Park, M., Randel, W. J., Kinnison, D. E., Bourassa, A. E., Degenstein, D. A., Roth, C. Z., McLinden, C. A., Sioris, C. E., Livesey, N. J.,  
305 and Santee, M. L.: Variability of Stratospheric Reactive Nitrogen and Ozone Related to the QBO, *Journal of Geophysical Research: Atmospheres*, 122, 10,103–10,118, <https://doi.org/10.1002/2017JD027061>, 2017.
- Prather, M. J.: Catastrophic loss of stratospheric ozone in dense volcanic clouds, *Journal of Geophysical Research: Atmospheres*, 97, 10 187–10 191, <https://doi.org/10.1029/92JD00845>, <https://agupubs.onlinelibrary.wiley.com/doi/abs/10.1029/92JD00845>, 1992.
- Preston, K. E., Jones, R. L., and Roscoe, H. K.: Retrieval of NO<sub>2</sub> vertical profiles from ground-based UV-visible measurements: Method  
310 and validation, *Journal of Geophysical Research: Atmospheres*, 102, 19 089–19 097, <https://doi.org/https://doi.org/10.1029/97JD00603>, <https://agupubs.onlinelibrary.wiley.com/doi/abs/10.1029/97JD00603>, 1997.
- Randel, W. J., Wu, F., Russell III, J. M., and Waters, J.: Space-time patterns of trends in stratospheric constituents derived from UARS measurements, *Journal of Geophysical Research: Atmospheres*, 104, 3711–3727, <https://doi.org/10.1029/1998JD100044>, <https://agupubs.onlinelibrary.wiley.com/doi/abs/10.1029/1998JD100044>, 1999.
- 315 Rieger, L. A., Zawada, D. J., Bourassa, A. E., and Degenstein, D. A.: A Multiwavelength Retrieval Approach for Improved OSIRIS Aerosol Extinction Retrievals, *Journal of Geophysical Research: Atmospheres*, 124, 7286–7307, <https://doi.org/10.1029/2018JD029897>, <https://agupubs.onlinelibrary.wiley.com/doi/abs/10.1029/2018JD029897>, 2019.
- Russell III, J. M., Gordley, L. L., Park, J. H., Drayson, S. R., Hesketh, W. D., Cicerone, R. J., Tuck, A. F., Frederick, J. E., Harries, J. E., and Crutzen, P. J.: The Halogen Occultation Experiment, *Journal of Geophysical Research: Atmospheres*, 98, 10 777–10 797,  
320 <https://doi.org/10.1029/93JD00799>, <https://agupubs.onlinelibrary.wiley.com/doi/abs/10.1029/93JD00799>, 1993.

SAGE III Algorithm Theoretical Basis Document, T.: SAGE III Algorithm Theoretical Basis Document (ATBD) Solar and Lunar Algorithm, Tech. rep., LaRC 475-00-109, <https://eosps0.gsfc.nasa.gov/sites/default/files/atbd/atbd-sage-solar-lunar.pdf>, 2002.

Sioris, C. E., Rieger, L. A., Lloyd, N. D., Bourassa, A. E., Roth, C. Z., Degenstein, D. A., Camy-Peyret, C., Pfeilsticker, K. E., Berthet, G., Catoire, V., Goutail, F., Pommereau, J.-P., and McLinden, C. E.: Improved OSIRIS NO<sub>2</sub> retrieval algorithm: description and validation, *Atmospheric Measurement Techniques*, 10, 1155 – 1168, <https://doi.org/10.5194/amt-10-1155-2017>, 2017.

325